Active and Passive Electronic Components,
September 2004, Vol. 27, pp. 125–131

Taylor & Francis
Taylor & Francis Group

STRUCTURAL, OPTICAL AND ELECTROCHROMIC PROPERTIES OF NANOCRYSTALLINE TiO_2 THIN FILMS PREPARED BY SPIN COATING

R. JOURDANI[a,*], A. OUTZOURHIT[a], A. OUERIAGLI[a], D. AITELHABTI[a], E. L. AMEZIANE[a], S. BARAZZOUK[b] and S. HOTCHANDANI[b]

[a]*Laboratoire de Physique des Solides et des Couches Minces, Faculté des Sciences Semlalia, B. P. 2390, Marrakech, Morocco;* [b]*Groupe de recherche en énergie et informations bio-moléculaires, Université de Québec à Trois Rivières, Bd. des Forges, CP500 G9A 5H7, Trois Rivières, Québec, Canada*

(Received 27 May 2003; In final form 28 July 2003)

Nanocrystalline TiO_2 thin films were prepared by spin coating on covered glass substrates with an indium tin oxide (ITO) layer. The structural, electrochromic and optical properties of the films were investigated. The films are crystallized predominantly in the anatase phase with lattice parameters $a = b = 0.378$ nm and $c = 0.958$ nm. The crystallite size was found to be of the order of 14 nm. The films showed reversible coloration/bleaching cycles as demonstrated by cyclic voltametry and current–time transients. The transmission of the blue colored films decreased and their absorption edge was less sharp and shifted to higher wavelengths as a result of the intercalation of Li^+ ions.

Keywords: Titanium oxide; Electrochromic films; Nanocristalline; Spin coating; Cyclic voltammetry; Optical transmission; Coloration/bleaching

1 INTRODUCTION

Recently, there has been a growing interest in nanomaterials due to their unique and varied properties as well as their high specific surface area. These materials have potential applications in dye-sensitized Gratzel-type solar cells [1–4], electrochromic devices [5], batteries and photo-catalysis [3, 4]. In particular, nanocrystalline TiO_2 has been extensively studied owing to its electrochemical stability [3, 6], its transparency in the visible spectral range and ease of fabrication [6].

Particularly, the electrochromic properties of polycrystalline thin films of transition element oxides or their solid solutions have been widely investigated due to their potential use in electrochromic devices and microbatteries [7]. These films have been prepared by a variety of techniques and can be colored at anodic potentials (*e.g.* Ni- and Ir-oxides) or cathodic potentials (*e.g.* W-, V-oxides) [7]. However, there have been only few reports on the electrochromic properties of TiO_2 thin films in general and of those of nanocrystalline films in particular.

* Corresponding author. Fax: (+212-44) 437410; E-mail: rjourdani@ucam.ac.ma

ISSN 0882-7516 print; ISSN 1563-5031 online
DOI: 10.1080/08827510310001616849

Indeed, Dinh *et al.* [8] have prepared nanocrystalline films by dip coating which showed good and reversible coloration/bleaching cycles in a 1 M $LiClO_4$ solution. However, the coloration time for these films is high (45 min) and the crystallite size is of the order of 40 nm.

In this work, we report on the structural, optical and electrochromic properties of nanocrystalline TiO_2 thin films prepared by spin coating from colloidal solutions of TiO_2.

2 EXPERIMENTAL PROCEDURE

The procedure followed to prepare nanocrystalline TiO_2 films was first described by Gregg *et al.* [9] and others [6, 10]. Briefly, a mixture of titanium VI isopropoxide (Aldrich) and 2-propanol (Aldrich) was added slowly to a glacial acetic acid solution under vigorous stirring. The solution is then heated to 80 °C while being stirred until its viscosity has noticeably increased. The heating was then interrupted and the viscous mixture is allowed to become a liquid. This cycle is repeated for 3–4 h until a colloidal solution is obtained. The solution is then placed in an autoclave and heated for 12 h at 230 °C. The resulting milky solution is used to prepare thin films by spin coating on either glass or ITO-coated glass substrates at a speed of 1800 rpm. The thin films are subsequently heat-treated at 400 °C for 1 h in air.

The structure of the obtained films was studied by X-ray diffraction using the CuKα radiation ($\lambda = 0.1542$ nm). Their microstructure was investigated by a scanning electron microscope (JEOL JSM5500). The optical transmission of the as-deposited and colored films was measured by a Shimadzu 3101-UVPC double-beam spectrophotometer in the wavelength range 200–3200 nm.

The electrochemical measurements were performed in a one-compartment cell where the thin film is the working electrode, a platinum sheet is the counter electrode and a saturated calomel electrode (SCE) is the reference. The electrolyte was a 1 M solution of $LiCO_4$ in propylene carbonate. The reference electrode was in contact with the electrolyte through a bridge containing the 1 M $LiClO_4$ solution.

3 RESULTS AND DISCUSSIONS

3.1 Crystalline Structure

A typical XRD spectrum of the obtained films on ITO-coated glass substrates is shown in Figure 1 together with that of the substrate for comparison. As can be seen, the spectrum is dominated by the characteristic peaks of the anatase phase of TiO_2. The other peaks are attributed to the substrate or to a minor rutile phase (weak and broad peak at $2\theta = 44.5°$). We note that the (101) peak of the anatase phase is the most intense and corresponds to an interplanar distance d of 0.353 nm. Furthermore, the peaks are large suggesting that the crystallite size is small. The latter is evaluated using the full width at half maximum (FWHM) of the (101) peak using Scherrer's formula given by:

$$\tau = \frac{0.9\lambda}{\beta \cos\theta} \tag{1}$$

where τ is the crystallite size, λ is the wavelength of the X-rays, β is the FWHM of the peak and θ represents the angular position of the peak. For the (101) peak located at $2\theta = 25.24°$, $\beta = 0.0103$ rad, and the resulting crystallite size is found to be $\tau \approx 14$ nm. This value is in accordance with that reported by Gregg *et al.* [9] and is lower than that of TiO_2 thin films

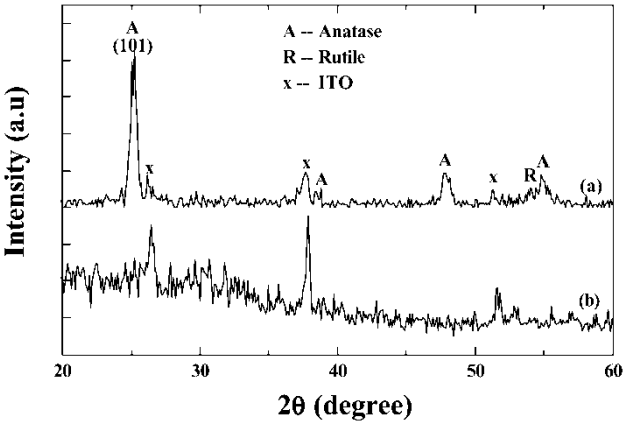

FIGURE 1 XRD spectra of a nanocrystalline TiO_2 thin film (a), and of an ITO-coated glass substrate (b).

prepared by rf sputtering [11, 12] or by dip coating [8]. The lattice parameters a and c were calculated from the position of the observed peaks and were found to be 0.378 and 0.958 nm, respectively. These results are in good agreement with those reported in the literature [8, 13].

A scanning electron micrograph of a drop of the colloidal solution deposited on a glass substrate and dried is shown in Figure 2. As can be seen, aggregates of particles which are a few nanometers in size are formed. This further supports the results obtained from the XRD measurements.

3.2 Electrochromic Properties

Figure 3 depicts the cyclic voltamograms of the as-prepared TiO_2 films in the -1500–0 mV/SCE voltage range and for various scan rates v_b (5, 20 and 50 mV/s). The as-deposited films were transparent and gave reversible cycles with a blue color at -1.2 V/SCE. The colored films become transparent upon applying voltages greater than -0.1 V/SCE. The

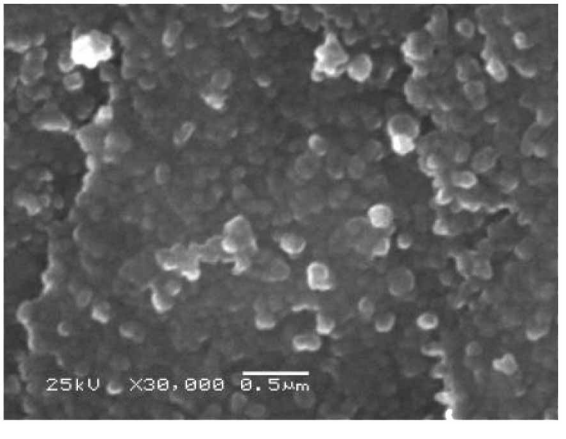

FIGURE 2 SEM micrograph of a TiO_2 thin film obtained by drying a drop of the colloidal solution on a glass substrate.

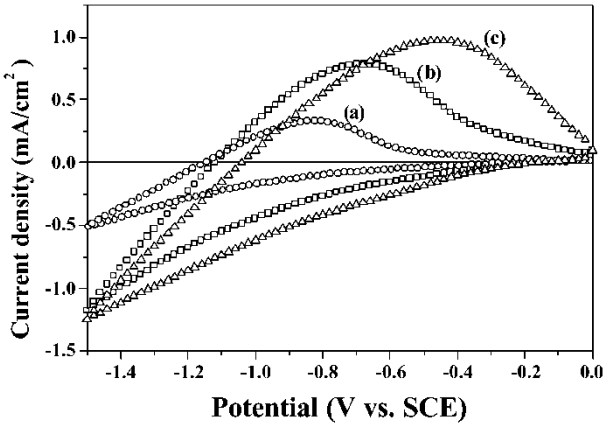

FIGURE 3 Cyclic voltammograms of colloidal TiO_2 thin films, at various scan rates: (a) 5 mV/s, (b) 20 mV/s and (c) 50 mV/s.

change in color is usually accompanied by the appearance of peaks in the cyclic voltamograms. In our case only the anodic peak can be clearly seen. The latter shifts towards more noble potentials as the scan rate (v_b) increases (Fig. 3). In addition, the corresponding current increases with increasing scan rate. Furthermore, a linear relationship between these parameters and $v_b^{1/2}$ was found, suggesting that the electrochromism in these films is diffusion controlled [14].

As reported in the literature [8, 14–19], the coloration of TiO_2 is a consequence of the simultaneous insertion of electrons and Li^+ ions into the film, leading to the reduction of Ti^{4+} to the Ti^{3+} state. It has also been reported that the progressive intercalation of Li^+ leads to the formation of an Li_xTiO_2 compound [14, 19]. On the other hand, the anodic peak corresponds to the oxidation of Ti^{3+} to Ti^{4+} accompanying the de-intercalation of Li^+ ions. The position of the anodic peak (-0.6 V at $v_b = 20$ mV/s) agrees with that found by other authors for the anatase phase [20].

Figure 4 also shows the coloration/bleaching cycles of TiO_2 films obtained by applying -1500 mV/SCE (injection) for 4 s and then -500 mV/SCE (extraction) for the same period of time. No significant change in the curves is observed after the second cycle. The initial current density during bleaching is always greater than that of the coloration, while the anodic current (bleaching) tends towards zero after 4 s suggesting that the extraction of the Li^+ ions is faster than their injection. This trend is also observed for longer cycles as shown in Figure 5. We can also deduce from this figure that the total charge injected during the coloration phase ($Q_c = 58$ mC/cm^2) is higher than that extracted during the anodic process ($Q_a = 8$ mC/cm^2) during the same time (15 min). These charges were evaluated from the areas under their respective curves (Fig. 5(a) and (b)). On the other hand, the comparisons of charges injected during 4 s and 15 min suggest that the intercalation process in our nanocrystalline films is slow. This behavior was also reported in amorphous or polycrystalline TiO_2 films prepared by other techniques [8, 20]. However, the coloration time of 15 min observed in films is lower than that of 45 min reported by some authors [8]. This may be attributed to smaller grain size and to the predominance of the anatase phase in our thin films. This time is, however, still higher than the coloration/bleaching time of 200 s observed in V_2O_5 thin films prepared by rf sputtering [21].

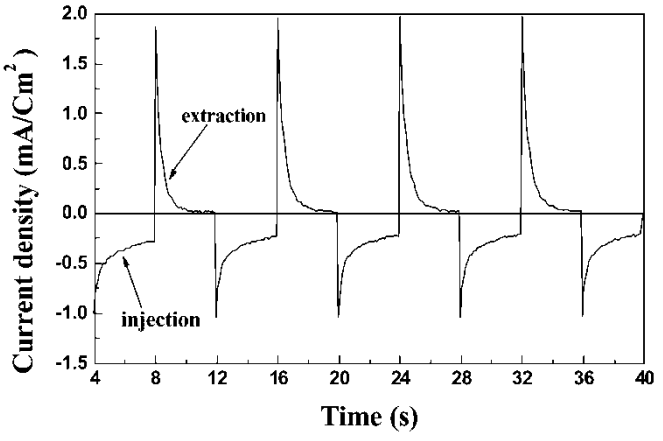

FIGURE 4 Typical coloration–bleaching cycles of a nanocrystalline TiO_2 thin film.

3.3 Optical Properties

Typical transmission spectra of TiO_2 films in the as-deposited, intensely blue colored and bleached states are represented in Figure 6. The as-deposited films on ITO-coated glass substrates (Fig. 6(a)) have a transmission exceeding 85% in the visible region, while the colored films have a 15% transmission in this wavelength range (Fig. 6(c)). After bleaching, the transmission of film (Fig. 6(b)) does not regain its initial value, which suggests that some Li^+ ions are still in the TiO_2 matrix [15]. This is in agreement with the differences observed in the measured anodic and cathodic charges.

Furthermore, the transmission of the film decreases and the absorption edge shifts to lower wavelengths and becomes less sharp upon coloration. These trends can be clearly seen in the absorbance spectra of these films shown in Figure 7. When polarized at -1500 mV (Fig. 7(c)), the films show a strong optical absorbance in the 300–800 nm wavelength range. When an anodic potential is applied (Fig. 7(b)), the absorbance decreases but does not reach the absorbance of the as-deposited film (Fig. 7(a)).

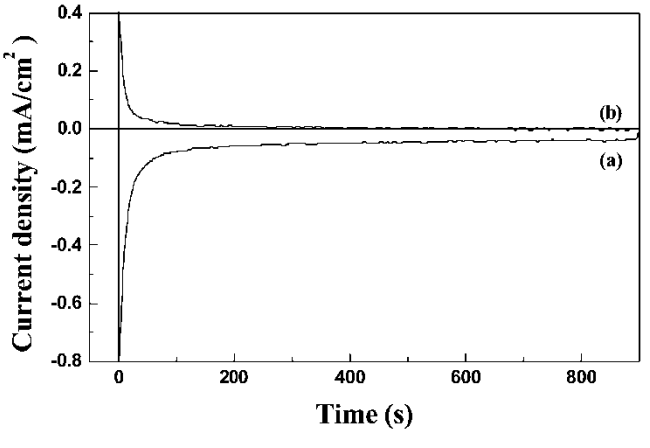

FIGURE 5 Time dependence of the current density during coloration at -1500 mV (a) and bleaching at -500 mV (b).

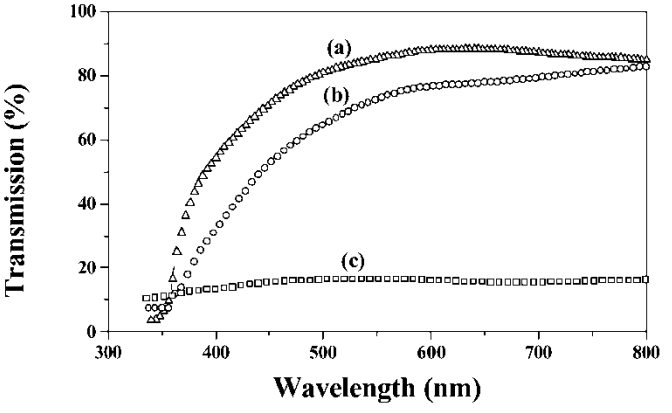

FIGURE 6 Transmission spectra of nanocrystalline TiO_2 thin films treated at various applied potentials: (a) as-deposited, (b) −500 mV, (c) −1500 mV.

The absorption coefficient α was extracted from the transmission of the films deposited on bare glass substrates from the region where the films absorb using the formula:

$$T = T_0 e^{-\alpha d}. \tag{2}$$

The curve $\alpha^{1/2}$ versus the photon energy hv, given in Figure 8, presents a linear region suggesting that the films are indirect band gap semiconductors. Indeed for such compounds the absorption coefficient is given by the formula:

$$\alpha = A(E_g - hv)^2 \tag{3}$$

where E_g is the optical band gap of the semiconductor, h is the Plank's constant and A is a constant. The extrapolation of this linear part to $\alpha = 0$ leads to an optical gap E_g of 3.4 eV for films deposited on glass substrates. This value is in close agreement with that reported by other authors [15].

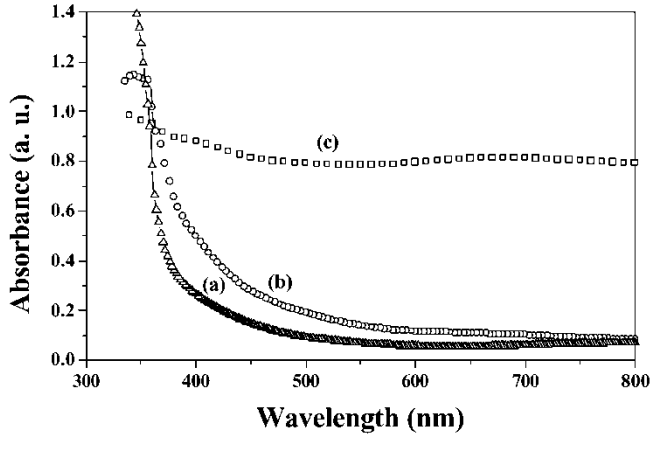

FIGURE 7 Absorption spectra of nanocrystalline TiO_2 thin films treated at various applied potentials: (a) as-deposited, (b) −500 mV, (c) −1500 mV.

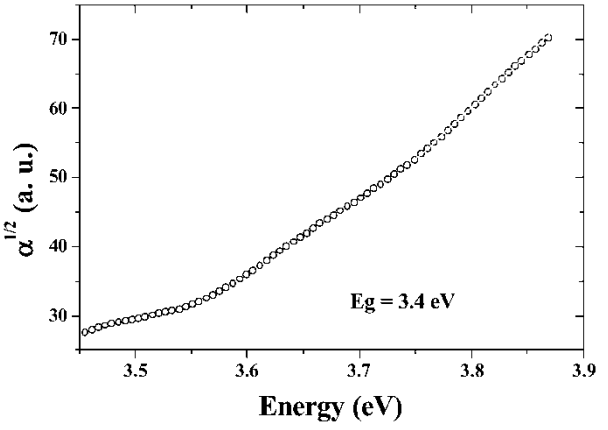

FIGURE 8 Square root of the absorption coefficient ($\alpha^{1/2}$) versus photon energy for nanocrystalline TiO_2 thin films deposited on a glass substrate (symbol) and a linear regression (line).

4 CONCLUSION

We have successfully prepared nanocrystalline TiO_2 films by spin coating of sol–gel derived colloidal solutions. The films are crystallized predominantly in the anatase phase with grain size of the order of 14 nm. The films showed improved electrochromic properties compared with previously reported films. Given the large coloration/bleaching times, which are not suitable for electrochromic displays, these films may be of interest in micro-batteries.

Acknowledgement

This work is supported by the PARS N° 60–physique and the FICU programs.

References

[1] O'Regan, B. and Grätzel, M. (1991). *Nature (London)*, **353**, 373.
[2] Hagfeldt, A., Vlachopoulos, N. and Grätzel, M. (1994). *J. Electrochem. Soc.*, **141**, L82.
[3] Kavan, L., Kratochilová, K. and Grätzel, M. (1995). *J. Electroanal. Chem.*, **394**, 93.
[4] Huang, S. Y., Kavan, L., Grätzel, M. and Exnar, I. (1995). *J. Electrochem. Soc.*, **142**, 142.
[5] Finklea, H. O. (1988). In: Finklea, H. O. (Ed.), *Semiconductor Electrodes.* Elsevier, Amsterdam, p. 44.
[6] Khazraji, A. C., Hotchandani, S., Das, S. and Kamat, P. V. (1999). *J. Phys. Chem. B*, **103**(2), 4693.
[7] Grandvist, C. G. (1995). In: *Handbook of Inorganic Electrochromic Materials.* Elsevier, Amsterdam, p.295.
[8] Dinh, N. N., Oanh, N. Th. T., Long, P. D., Bernard, M. C. and Hugot-Le Goff. (2003). *Thin Solid Films*, **423**, 70–76.
[9] Zaban, A., Ferrere, S., Sprague, J. and Gregg, B. A. (1997). *J. Phys. Chem. B*, **101**, 55–57.
[10] Nazeeruddin, M. K., Liska, P., Moser, J., Vlachopoulos, N., Grätzel, M. (1990). *Helv. Chim. Acta*, **73**, 1788.
[11] Gomez, M., Rodriguez, J., Lindquist, S.-E. and Granqvist, C. G. (1999). *Thin Solid Films*, **342**, 148–152.
[12] Mardare, D., Tasca, M., Delibas, M. and Rusu, G. I. (2000). *Applied Surface Science*, **156**, 200–206.
[13] ASTM Powder Diffraction Data Cards. International Center for Diffraction Data, New York, 1969.
[14] Granqvist, C. G., Azens, A., Isidorsson, J., Kharrazi, M., Kullman *et al.* (1997). *J. Non-Crystalline Solids*, **218**, 273.
[15] Natarajan, C. and Nogami, G. (1996). *J. Electrochem. Soc.*, **143**(5), 1547.
[16] Ye Yonghong, Zhang Jiayu, Gu Peifu, Liu Xu and Tang Jinfa (1997). *Thin Solid Films*, **298**, 197.
[17] Krtil, P., Fattakhova, D., Kavan, L., Burnside, S. and Grätzel, M. (2000). *Solid State Ionics*, **135**, 101–106.
[18] Kullman, L., Azens, A. and Granqvist, C. (1997). *J. Appl. Phys.*, **81**, 8002.
[19] Özer, N. (1992). *Thin Solid Films*, **214**, 17.
[20] Zhongchun Wang and Xingfang Hu (1999). *Thin Solid Films*, **352**, 62–65.
[21] Benmoussa, M., Outzourhit, A., Bennouna, A. and Ameziane, E. L. (2002). *Thin Solid Films*, **405**, 11.